Static Properties of Homopolymer Melts in Confined Geometries Determined by Monte Carlo Simulation

R. S. Pai-Panandiker and J. R. Dorgan*

Department of Chemical Engineering, Colorado School of Mines, Golden, Colorado 80401

Tadeusz Pakula

Max-Planck-Institut für Polymerforschung, Ackerman Weg 10, D-55021, Mainz, FRG

Received December 17, 1996; Revised Manuscript Received July 10, 1997[⊗]

ABSTRACT: The static properties of a homopolymer melt between energetically neutral walls are studied as a function of the degree of confinement (plate spacing) and polymer molecular weight. The cooperative motion lattice model is used and allows all calculations to be performed at full occupancy (i.e., at a volume fraction of 1); chain lengths varying from 384 to 24 are examined. Properties investigated include the magnitude of the end-to-end vector, the radius of gyration, and components of the end-to-end vector. In addition, orientation effects and the distribution of chain ends are also calculated. As the chains are confined, the end-to-end vectors align parallel to the walls beginning at a value of about twice the unconstrained value of the radius of gyration, regardless of the molecular weight. For values less than this, chain conformations are distorted and the magnitude of the average end-to-end vector and radius of gyration increase. The components of the end-to-end vector parallel and perpendicular to the walls are considered; in the cases of confinement, it is seen that there is a universal scaling relationship between the parallel component of the end-to-end vector and the plate spacing. The parallel component increases with the decreasing plate spacing according to approximately a one-sixth power ($\langle r^2\rangle_{\parallel}^{1/2} \sim L^{-1/6}$). Chain ends are most likely to be in the vicinity of one of the walls due to entropic constraints.

1. Introduction

A fundamental understanding of the behavior of polymer melts in confined geometries is of interest for both theoretical and practical purposes. Widespread applications involving confined polymers appear in fields varying from molecular biology to enhanced oil recovery. These include the separation of proteins by gel filtration, the use of polymer additives in enhanced oil recovery, and the addition of polymers to many lubricants. In these (and many other) applications the polymer chains are confined to small dimensions that perturb their normal static properties. In fact, the molecules at the free surface of any part made from a polymeric material are confined to the polymer−air interface.

Applications involving the coextrusion of polymeric materials necessitate the interdiffusion of chains residing at the two interfaces for the sake of mechanical integrity. Of particular interest in this case is the distribution of chain ends in the near surface region that controls the interdiffusion rate.[1] Knowledge of the chain end distribution near a bounding interface is relevant to polymer welding and adhesion issues. These, and other technical issues, may be addressed through the use of molecularly detailed Monte Carlo generated lattice models.

The conformational behavior of polymer chains contacted by a solid surface is distinct from their bulk properties. In the presence of an interface, the normally disordered chemical bond orientations of a macromolecule exhibit an ordering tendency with respect to the wall. For the confined case similar behavior has been found; bulk properties are realized only when confinement is larger than the unperturbed conformational dimensions.

Several investigations have focused on studies of the conformational behavior of polymers between flat plates. Analytical lattice models have been used to treat this problem using mean field approximations.[2] Mansfield and Theodorou used a lattice Monte Carlo simulation method to demonstrate that the microscopic structure of a polymer melt is significantly affected by the presence of solid walls.[3] Flattened chain conformations in the vicinity of the walls, variation in the segmental density, and increased chain relaxation times were found. Other researchers used a continuous space (nonlattice) Monte Carlo method and have presented consistent results; they also reported an enhancement in the chain end concentration near the walls.[4] Kumar et. al. have also used off-lattice Monte Carlo simulations and predicted that the effect of the presence of the walls is confined to those segments that lie within a distance from the walls of approximately two radii of gyration.[4−6] These researchers also predicted an enhancement of chain ends in the vicinity of the walls and a dependence on the chain length of the density of chain ends at the walls. This reported dependence contrasts with the lattice Monte Carlo results of ten Brinke et al., who found no dependence on either the chain length or the plate separation.[7] On-lattice Monte Carlo studies due to Wang and Binder support the chain length dependence of the density of chain ends at the walls.[8] Binder et al. have also reported Monte Carlo results for chains confined to a tube with attractive walls.[9] On-lattice Monte Carlo simulations by Pakula have also investigated the effects of confinement on linear chains and shown that linear chains can be represented by a cigarlike shape and that the presence of the walls influenced the orientation of the cigar, but not the shape of the cigars.[10,11]

Experimental results on confined polymer chains and chain end distribution have been minimal. However, it was known that the surface tension of alkanes and oligomers is chain length dependent and this fact has been attributed to the concentration of chain ends at the fluid surface.[12] Theoretical results have sought to quantitatively explain these phenomena.[13] Recently,

[⊗] Abstract published in *Advance ACS Abstracts,* September 1, 1997.

S0024-9297(96)01858-X CCC: $14.00

direct experimental measurements on confined chains have been performed.[14] The force−distance profile to compress a homopolymer between two plates and the oscillatory shear responses at molecular dimensions were measured, and an enhancement of chain entanglements was inferred. Simulation results of Shaffer imply that invoking an entanglement enhancement to explain these experiments is not necessary.[15]

Most of the Monte Carlo work performed to date uses methods that rely on reduced densities. In this paper, the effects of confinement on the conformational properties of a polymer melt trapped between hard, neutral walls at *full occupancy* are studied. Unlike many previous studies, the segmental density near the wall cannot increase and the melt is fully incompressible. Orientational effects due to true chain confinement are thus calculable as a function of plate spacing. The cooperative motion Monte Carlo algorithm is used to obtain detailed information about the behavior of these dense systems.[16,17]

The present study demonstrates that effects of confinement on chain conformation are observed when the wall-to-wall separation distance goes below about twice the free chain radius of gyration ($\langle s^2\rangle_0^{1/2}$); below this spacing there is a distinct tendency for chain orientation. For the smaller wall separation distances, the average end-to-end vector of the polymer chains is strongly oriented in a direction parallel to the walls. The component of the end-to-end vector parallel to the walls is then considered; it is found that this component increases with decreasing plate spacing according to approximately a one-sixth power. This behavior is seen to be true in the presence and absence of solvent, for all chain lengths, under the constraint of confinement. Furthermore, studies on the distribution of chain ends indicate an increased likelihood of finding a chain in the vicinity of one of the plates. A chain length dependence of the density of chain ends at the walls is also found.

2. The Simulation Method

The cooperative motion algorithm is used to perform the Monte Carlo moves for the polymer chains residing on a face centered cubic (FCC) lattice. The bond lengths are constant and equal to $\sqrt{2}a$, where a is the lattice constant. The permissible bond angles are 180°, 120°, 90°, and 60° and the coordination number for the FCC lattice is 12. The idea of the algorithm is to simulate motions in a system by rearranging several chain segments collectively. Each chain segment moved replaces its nearest neighbor along a closed path. The collective motion of beads is subject to certain rules; the motions are performed such that the chain connectivity, sequencing of segments, chain lengths, and bond lengths are preserved. The algorithm results in rearrangement paths that are random, non-self-avoiding, closed walks of relatively broad length distributions. Further details of the algorithm are found in earlier works.[16,17]

In the simulation box, the solid walls reside at $x = 0$ and $x = L$ while periodic boundary conditions are imposed in the y and z directions. The homopolymers are thus confined between two walls, but the simulation box remains infinite in the plane of the walls. Chain lengths and box dimensions are chosen in order to meet the requirement that every site in the lattice is filled. Polymer chains that were studied have lengths varying between 384 and 24 segments, and the plate spacing is varied from 48 to 2 lattice sites. The simulations are run at volume fractions of 0.25, 0.5, 0.75, and 1.0. It is noted that simulations in a partially filled lattice correspond to conformations in an athermal solvent. The walls are modeled as hard, impenetrable surfaces, and the polymer segments are modeled as hard sites. Enthalpic effects are not considered, making the simulations representative of a polymer melt between neutral walls. The simulation consists of three phases: the generation of the initial configuration, equilibration of the structure, and analysis of the data.

The initial configuration is generated as an FCC crystal with every site being occupied. The chains are initially laid out in an all trans conformation. Monte Carlo moves are then performed in accordance with the algorithm, and the system is equilibrated to ensure that the effect of the initial configuration is lost before calculating properties. The end-to-end distance ($\langle r^2\rangle^{1/2}$) and the radius of gyration ($\langle s^2\rangle^{1/2}$) are followed as a function of the number of Monte Carlo moves until they reach equilibrium values. The simulation trajectory is followed by tracking the conformational properties.

Data analysis includes the accumulation and averaging of the equilibrated $\langle r^2\rangle^{1/2}$ and $\langle s^2\rangle^{1/2}$ as a function of plate spacing. Furthermore, the orientation of the average end-to-end vector is determined by calculation of the various order parameters with respect to the different axes, f_x, f_y, f_z (subscripts indicate reference axis). The values of the end-to-end distance ($\langle r^2\rangle^{1/2}$) and the radius of gyration ($\langle s^2\rangle^{1/2}$) along with the order parameters (f_x, f_y, f_z) enable the determination of the parallel ($\langle r^2\rangle_{\|}^{1/2}$) and perpendicular ($\langle r^2\rangle_{\perp}^{1/2}$) components of the end-to-end vector.

3. Results and Discussions

The mean squared end-to-end distance ($\langle r^2\rangle$) is calculated according to

$$\langle r^2\rangle = \langle (r_{\mathrm{N},i} - r_{\mathrm{l},i})^2\rangle \tag{1}$$

In the above equation, $r_{\mathrm{N},i}$ indicates the spatial position of the last site on chain i and $r_{1,i}$ indicates the position of the first site on chain i. The mean squared radius of gyration ($\langle s^2\rangle$) is calculated from

$$\langle s^2\rangle = \left\langle \frac{1}{N}\sum_j (r_j - r_{\mathrm{cm}})^2 \right\rangle \tag{2}$$

Here, r_j is the position of the jth site on a chain, r_{cm} is the position of the center of mass of the chain, and N is the number of segments in the chain. The values of $\langle r^2\rangle_0$ and $\langle s^2\rangle_0$ are calculated for chains of different lengths at unconstrained conditions ($L >> \langle r^2\rangle^{1/2}$). The ratio of $\langle r^2\rangle_0/\langle s^2\rangle_0$ is found to be 6.00 ± 0.20 for all molecular weights investigated. This is in accordance with the well-known relationship for ideal Gaussian chains given by eq 3. For the purpose of this article, the subscript "0" is used to denote the unconstrained, unconfined case.

$$\langle s^2\rangle_0 = \frac{1}{6}\langle r^2\rangle_0 \tag{3}$$

The scaling behavior described by the law $\langle s^2\rangle^{1/2} \sim N^{\nu}$ is verified; for the unconstrained case, a scaling exponent of 0.51 and a primitive step length of 1.57 is obtained. The exponent agrees with the ideal scaling exponent of 0.50 for a homopolymer melt. The effective primitive step length of the model is calculated by averaging over the permissible bond angles and lengths

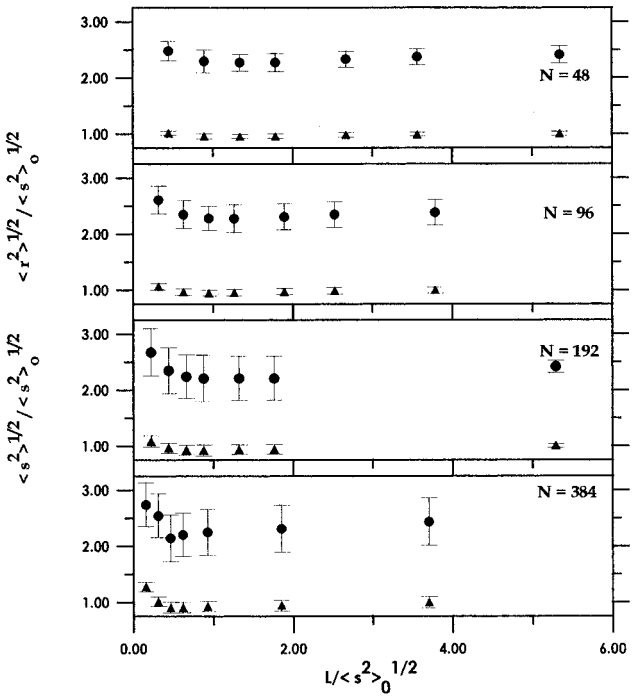

Figure 1. Normalized chain dimensions, $\langle r^2\rangle^{1/2}/\langle s^2\rangle_0^{1/2}$ (●) and $\langle s^2\rangle^{1/2}/\langle s^2\rangle_0^{1/2}$ (▲), as a function of plate spacing for chain lengths of 48, 96, 192, and 384 segments. Error bars show 95% confidence limits.

on the lattice and is 1.58. This value compares well with the simulation result of 1.57 and implies that all bond angles are equally populated under unconfined conditions.

Figure 1 is a plot of the end-to-end distance and radius of gyration versus plate spacing for various chain lengths. In this plot, all quantities are normalized by the value of the unconstrained radius of gyration for the chain length under consideration. The effect of confinement clearly becomes significant as the plate spacing is reduced to below the value of the unconstrained radius of gyration ($\langle s^2\rangle_0^{1/2}$). It is noted, however, that as the plate spacing is decreased, there exists a small "dip" in the chain dimensions in the vicinity of $L \sim \langle s^2\rangle_0^{1/2}$. This is due to the fact that as confinement is increased, the chains encounter the presence of reflecting walls and hence fold back onto themselves, resulting in a decrease in chain dimensions. However, as the chains are further confined, chains must enlarge in directions parallel to the plates due to the requirement of full occupancy, thus resulting in an eventual increase in chain dimensions. At plate spacings less than a single radius of gyration, chain conformations are strongly distorted from their unconstrained values. The chains stretch to values of the end-to-end distance of between 2 and 3 times the unconstrained value. The magnitude of this enhancement increases with increasing molecular weight as expected.

Ordering effects of confinement are found by calculating the order parameters defined by

$$f_i = \frac{1}{2}\langle 3\cos^2\theta_i - 1\rangle \tag{4}$$

Where f_i represents the order parameter in the direction of the ith-axis ($i = x, y, z$) and θ_i represents the angle made by the end-to-end vector with the i-axis. Values of the order parameters range from −0.5 to +1.0; a value of −0.5 implies perpendicular alignment, while a value

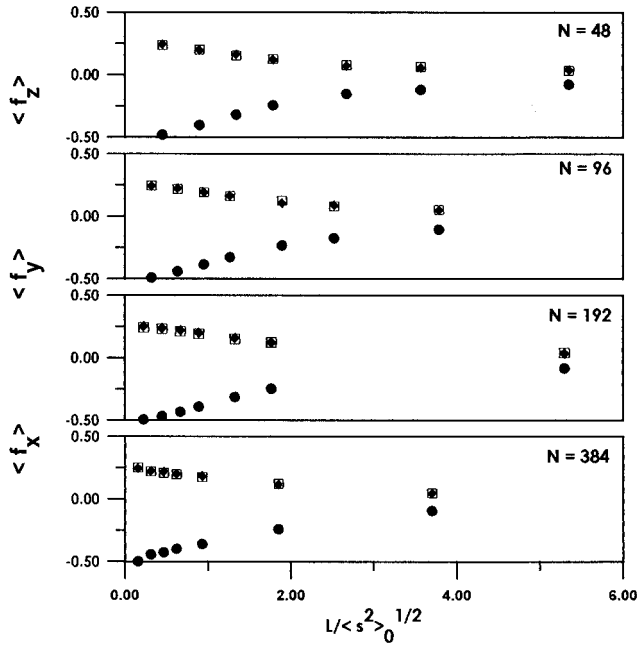

Figure 2. Order parameters, f_x (●), f_y (□), and f_z (♦), as a function of plate spacing for chain lengths of 48, 96, 192, and 384 segments.

of 1.0 implies parallel alignment with the respective axis. It is pointed out that the walls themselves are perpendicular to the x-axis and hence chains oriented perpendicular to the x-axis are parallel to the walls.

Figure 2 demonstrates that as the plate separation distance is reduced, the orientation parameter in the direction perpendicular to the wall, f_x, tends toward a value of −0.5 while f_y and f_z tend toward positive values, clearly indicating a tendency for the chains to lie parallel to the walls. It is also noted that the unconfined values of the order parameters approach zero, indicating little preferential orientation. This slight deviation from zero with the plates well separated is due to the preferential orientation imposed by the reflecting walls on the chains near the walls. As the plates are brought together, the end-to-end vectors align parallel to the walls, beginning at a value of approximately twice the unconstrained value of the radius of gyration, regardless of the molecular weight.

The parallel component of the end-to-end vector ($\langle r^2\rangle_{||}^{1/2}$) is defined as the sum of the components of the end-to-end vector in the directions parallel to the walls (corresponding to the y- and z-axes in the simulation box).

$$\langle r^2\rangle_{||}^{1/2} = (\langle r_y^2\rangle + \langle r_z^2\rangle)^{1/2} \tag{5}$$

The perpendicular component of the end-to-end vector ($\langle r^2\rangle_{\perp}^{1/2}$) is defined as the component of the end-to-end vector in the direction perpendicular to the walls (x-axis).

$$\langle r^2\rangle_{\perp}^{1/2} = (\langle r_x^2\rangle)^{1/2} \tag{6}$$

The chains are severely flattened and elongated as the plate spacing is reduced. This is evident in Figure 3, which shows the drastic increase in the parallel component and reduction of the perpendicular component as the plates are brought together.

The end-to-end vector and order parameters are used to determine the average magnitude of the parallel and

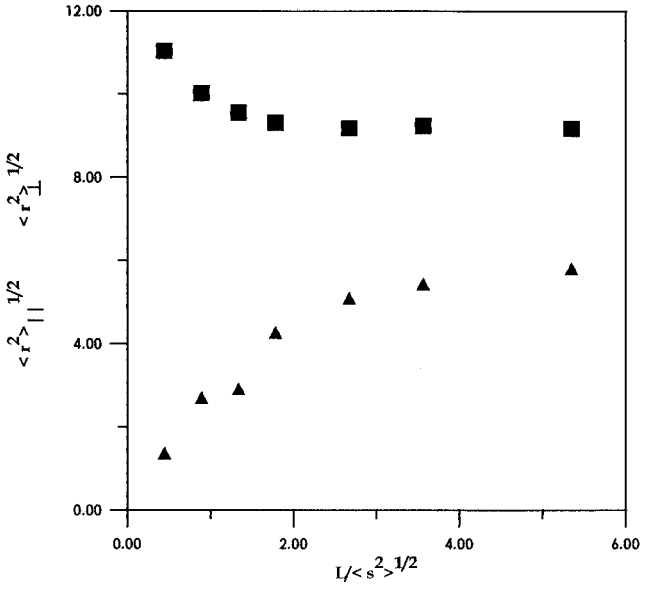

Figure 3. The parallel, $\langle r^2\rangle_{||}^{1/2}$ (■), and perpendicular, $\langle r^2\rangle_{\perp}^{1/2}$ (▲), components of the end-to-end vector as a function of plate spacing for a chain length of 48 segments.

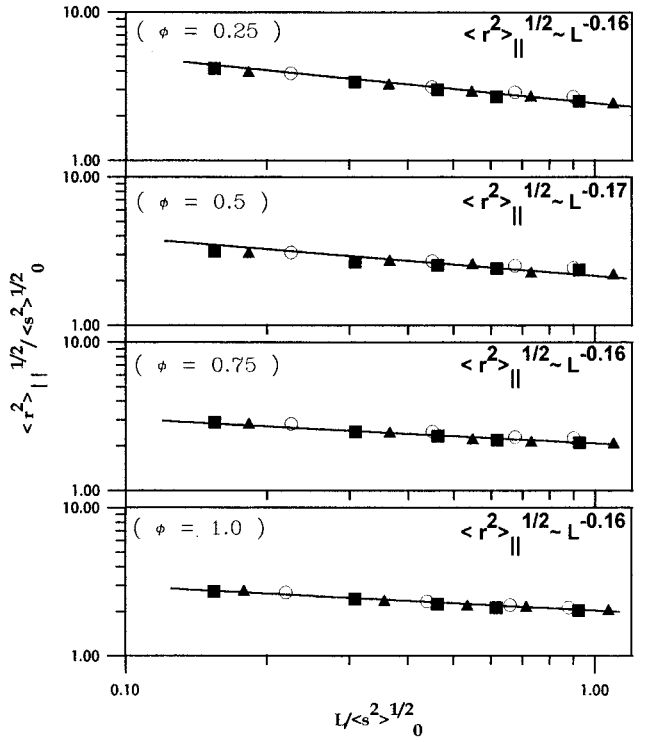

Figure 4. Scaling behavior of the parallel component of the end-to-end vector, $\langle r^2\rangle_{||}^{1/2}$ (N = 192 (○), N = 288 (▲), N = 384 (■)), as a function of normalized plate spacing for chains of length 192, 288, and 384 segments for volume fraction of polymer ϕ = 1.00, 0.75, 0.50, and 0.25.

perpendicular components of the end-to-end vector ($\langle r^2\rangle_{||}^{1/2}$ and $\langle r^2\rangle_{\perp}^{1/2}$). A plot of the normalized parallel component, $\langle r^2\rangle_{||}^{1/2}$, for different chain lengths, against the normalized plate spacing is shown in Figure 4. This plot incorporates polymer chains at different volume fractions, ϕ, in an athermal solvent. The slope of this plot is -0.165 ± 0.005, which is extraordinarily close to $-1/6$. The coefficient of determination for the regression is $R^2 = 0.99$. This implies that there is a universal scaling relationship between the parallel component of the end-to-end vector and the normalized plate spacing; the parallel component of the end-to-end vector increases with decreasing plate spacing in accordance with the relationship

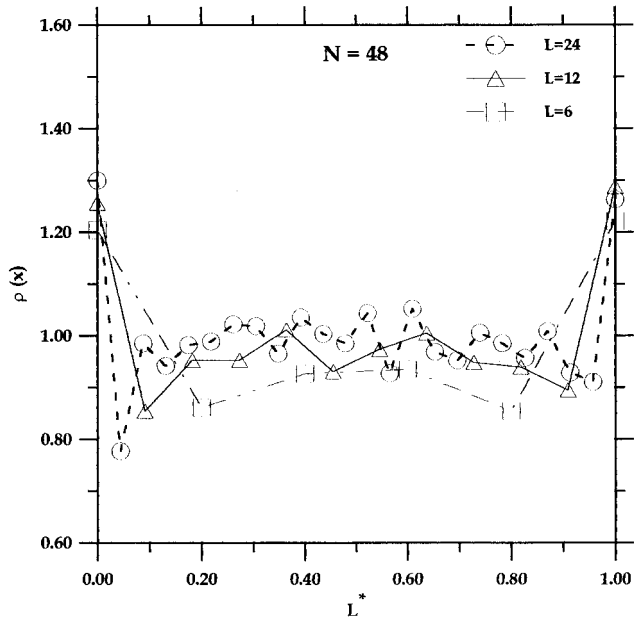

Figure 5. Normalized distribution of chain ends, $\rho(x)$, as a function of normalized plate spacing, L^*, for chains of length 48 segments.

$$\langle r^2\rangle_{||}^{1/2} \sim L^{-1/6} \tag{7}$$

where L is the plate spacing. Scaling relationships for chains confined to capillaries (one dimension, $\langle r^2\rangle_{||}^{1/2} \sim L^{-2/3}$) and strips (two dimensions, $\langle r^2\rangle_{||}^{1/2} \sim L^{-1/3}$) are known.[18] However, this $^1/_6$th scaling law for three-dimensional confinement between plates is previously unreported.

The normalized chain end density in any x-layer, is given by[8]

$$\rho(x) = \frac{N}{2}\frac{\phi_e(x)}{\phi(x)} \tag{8}$$

where N is the number of chain segments per chain, $\phi_e(x)$ is the number of chain ends in the layer, x, and $\phi(x)$ is the total number of monomers in the layer, x. In an isotropic melt, the normalized chain end density corresponds to a value of unity. The normalized chain end density at the walls is denoted by $\rho(1)$ and $\rho(L)$. The normalized plate spacing, L^*, is given by

$$L^* = \frac{(x - x_{MIN})}{(x_{MAX} - x_{MIN})} \tag{9}$$

where x corresponds to the specific layer, x_{MIN} represents the value of the first layer (equal to 1), and x_{MAX} represents the specific plate spacing, L.

Figure 5 is a representative plot of $\rho(x)$ versus L^* for the cases of homopolymer melts of chains of 48 segments in length. Results for plate spacings of L = 24, 12, and 6 are shown; in all cases (chain lengths of 48, 96, 144, 192, and 384) there is a preference for the chain ends to be in the layer adjacent to the wall. A preference for ends to reside at the walls implies that the entropic constraint of the impenetrable surface is less severe for an end segment than it is for a segment in the main backbone of the polymer chain. Within 95% confidence limits, there is no discernible dependence of $\rho(x)$ on

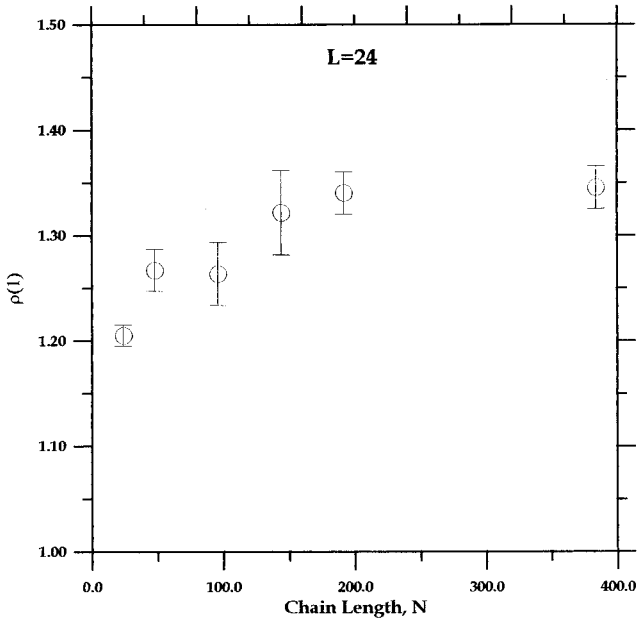

Figure 6. Normalized chain end distribution at the walls, $\rho(1)$, versus chain length, N. Error bars indicate 95% confidence limits.

confinement. Conservation of chain ends requires that enhancement at the walls is compensated for by depletion elsewhere. In the case of no confinement, the enhancement of chain ends at the walls propagates for approximately one radius of gyration of free chains. Beyond one radius of gyration, the perturbation effect is lost and the chains behave isotropically. However, in the case of extreme confinement, the plate spacing is low enough that the perturbation effects of end enhancement produce a depletion region throughout the plate separation region.

A dependence of $\rho(1)$ on chain length is evident in Figure 6. At higher chain lengths, $\rho(1)$ reaches an asymptotic value, suggesting an exponential form of dependence; this result is in agreement with previous works.[6,8]

4. Conclusions

Monte Carlo simulations of a homopolymer melt confined between two neutral walls at full occupancy demonstrate that the end-to-end vector and the radius of gyration ($\langle s^2 \rangle^{1/2}$) are profoundly altered from their bulk values. Distortion effects become evident when the plate spacing reaches a value corresponding to about twice the value of the unconstrained radii of gyration of the chains, irrespective of the molecular weight. For plate spacings on the order of the radius of gyration, chain dimensions are slightly reduced; however, in the case of extreme confinement the dimensions grow larger as a result of their excluded volume. The usual one-half scaling exponent for the radius of gyration and the end-to-end vector versus the chain length is obtained. Also, there is a dramatic increase in the component of the end-to-end vector in the direction parallel to the walls and a reduction in the perpendicular component. This flattening-of-the-chains phenomenon is corroborated by a study of the order parameters. As confinement increases, the chain order parameter in the direction perpendicular to the walls, f_x, tends toward a value of -0.5, while those parallel to the walls, f_y and f_z, tend toward 1.0, indicating that on average the chains are parallel to the plates or in a flattened conformation. The end-to-end vector and order parameters allow calculation of parallel and perpendicular components of the end-to-end vector. There is a universal scaling relationship between the parallel component of the end-to-end vector and the plate spacing (i.e., as the plate spacing decreases, the parallel component of the end-to-end vector increases with the one-sixth power of the plate spacing). This apparent scaling remains unexplained.

The distribution of chain ends is also studied. An increased likelihood of chain ends residing at one of the walls is observed. This demonstrates that it is entropically favorable for chain ends to be at the walls compared to a backbone segment. Further analysis shows that the chain end density reaches an asymptotic value of 1.35. The increased maximum chain dimensions are realized through preferential bond orientation with the walls. In this work, the effects of confinement on static properties under the conditions of full occupancy have been further elucidated.

Acknowledgment. This work has been supported by the National Science Foundation under career award CTS-9502466.

References and Notes

(1) Stamm, M. *Adv. Polym. Sci.* **1992**, *100*, 357.
(2) DiMarzio, E. A.; Rubin, R. J. *J. Chem. Phys.* **1971**, *55*, 4318.
(3) Mansfield, K. F.; Theodorou, D. N. *Macromolecules* **1989**, *22*, 3143.
(4) Yethiraj, A.; Hall, C. K. *Macromolecules* **1990**, *23*, 1865.
(5) Kumar, S. K.; Vacatello, M.; Yoon, D. Y. *J. Chem. Phys.* **1988**, *89*, 5206.
(6) Kumar, S. K.; Vacatello, M.; Yoon, D. Y. *Macromolecules* **1990**, *23*, 2189.
(7) ten Brinke, G.; Ausserre, D.; Hadziioannou, G. *J. Chem. Phys.* **1988**, *89*, 4374.
(8) Wang, J. S.; Binder, K. *J. Phys. I* **1991**, *1*, 1583.
(9) Milchev, A.; Paul, W.; Binder, K. *Macromol. Theory Simul.* **1994**, *3*, 305.
(10) Pakula, T. *J. Chem. Phys.* **1991**, *95*, 6, 4685.
(11) Pakula, T.; Zhulina, E. B. *J. Chem. Phys.* **1991**, *95*, 6, 4691.
(12) Koberstein, J. T., In *Encyclopedia of Polymer Science and Engineering*, Mark, H. F., Bikales, N. M., Overberger, C. G., Menges, G., Eds.; Wiley: New York, 1987; Vol. 8.
(13) Wu, D. T.; Fredrickson, G. H.; Carton, J.-P.; Adjari, A.; Leibler, L. *J. Polym. Sci., Part B: Polym. Phys.* **1995**, *33*, 2373.
(14) Hu, H.-W.; Granick, S.; Schweitzer, K. S. *J. Non-Cryst. Solids* **1994**, *172−174*, 721.
(15) Shaffer, J. S. *Macromolecules* **1996**, *29*, 1010.
(16) Pakula, T. *Macromolecules* **1987**, *20*, 679.
(17) Gauger, A.; Weyersberg, A.; Pakula, T. *Makromol. Chem., Theory Simul.* **1993**, *2*, 531.
(18) Wall, F. T.; Seitz, W. A.; Chin, J. C.; deGennes, P. G. *Proc. Natl. Acad. Sci. U.S.A.* **1978**, *75*, 2069.

MA9618585